



AC/DC Interlinking Converter for the EVs Charging Station

Yashpal Kushwaha¹, Sachindra Verma²

¹ Student NRI Institute of Research and Technology, Bhopal

² Professor NRI Institute of Research and Technology, Bhopal

ABSTRACT—

For vehicles charger stage, to meet the dynamic power demands of EVs; while, keeping the balance between available generation amounts, interleave converter is proposed combined to sub-management strategy. The proposed conversion stage and management address the low depending on grid sources for the charging purposes when, peak load is present at the grid side. Hence, the proposed charging strategy greatly decreases the stress on grid especially at peak hours. To operate the system under desirable conditions, a rule-based management strategy (REMS) is proposed. This interactive strategy with limits in response time strategy, initializing from maximized utilization of PV source, then using BSS to supplement power and utilizing grid during intermittent conditions affecting PVs. The management strategy ensures reliable operation of system, while maximizing the PV utilization, meeting the EVs demand and maximizing the life the BSS. In this thesis, a hybrid charging system based on PV, BSS and conventional grid is proposed to support the needs of EVs load. Efficient energy conversion stage is proposed using interleaved buck-boost converters to improve the quality of power. State of charge estimation (SoC) of lithium-ion battery using an extend Kalman filter (EKF) is proposed. On-line management strategy is developed to maximize the renewable energy utilization, to insert lesser stress on grid and to improve the utilization of BSS.

Keywords— Electric vehicle charging station, power conversion stages, battery modelling energy management system

Introduction

People need cars to travel about and move things, which is why oil is always in demand. People are frightened because of increased demand, rising fuel prices, and growing concerns around the world about climate change and air pollution. Because of this, several governments have instructed vehicle companies to build cars that are better for the environment and make less pollution [1]. In this case, electric vehicles (EVs) have been made and employed to help us use less fossil fuels. Because of this, greenhouse gases and other pollutants are being released less [2]. There are also restrictions about vehicle emissions to safeguard the environment from damage caused by normal cars [3]. The US, the UK, Japan, and Europe are just a few of the countries that have set standards for transportation systems to cut down on automobile emissions. Since the Euro 5 emission rules went into effect, the net percentage of "atmospheric aerosol particles" generated by car exhaust has dropped by 99%. Since the Euro 1 emission standard, levels of carbon dioxide and nitrogen dioxide have also gone down a lot. But in Europe, they intend to lower nitrogen dioxide emissions from cars by 35 mg/km and carbon dioxide emissions by 95 g/km by 2020.

The cost of the electrical elements needed to change the energy makes the rapid charger a more expensive option for an EV overall. But on-board chargers can't charge EVs quickly since the power electronics that come with the EV are quite expensive and the charger in the car needs to be bigger. People utilize off-board chargers that give off a lot of DC power to make sure that EVs charge quickly [2, 18]. Keep in mind that each off-board charger has its own converter that changes AC to DC power. To make sure the car charges quickly, it's vital to boost the power of the converters. The findings from 14 published studies have been utilized to create EV charging stations that are both effective and dependable. It is important to think about the idea of a public place with high-power off-board chargers that works as a charging station. This kind of station can charge electric vehicles' batteries quickly and give them the same services as a petrol station by delivering them direct current [19, 20]. There are only two types of charging station architecture that need to be connected to a grid: AC and DC. In the first architecture, the secondary side of the step-down transformer acts as a shared AC bus. Each load is connected to the bus through its own AC/DC stage. In the second architecture, one AC/DC stage is set up to provide a common DC bus service for the system load [21, 22].

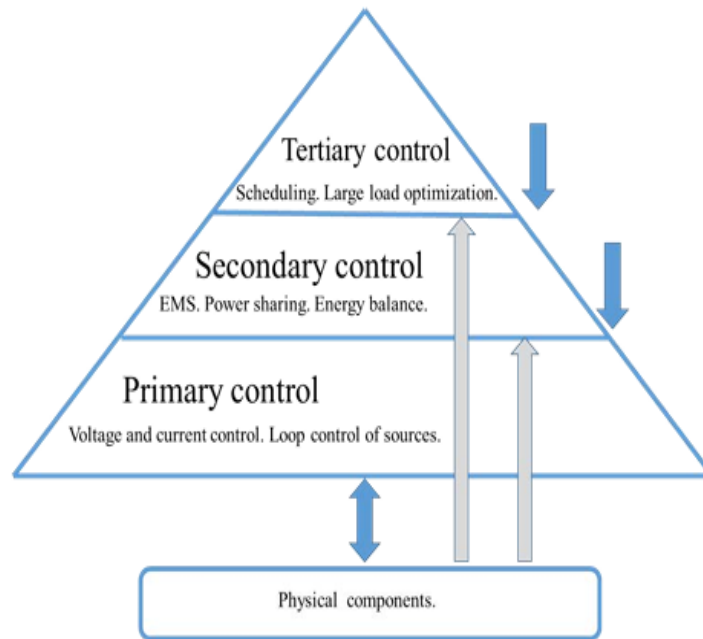


Figure 1. Hierarchical control of EV charging station

Interleaved boost converter for PV system

Generally, the DC/DC boost converter is used to connect the PV panel to the DC bus thanks to its simplicity. Meanwhile, it is used for the battery with converter in bidirectional mode. However, several drawbacks concerning this topology in terms of vehicle battery charging applications should be considered, mainly: (i) low efficiency for high voltage gains; (ii) low elevation gain; (iii) weight and volume of the inductance (low compactness); (iv) high current ripple; (v) sensitivity to faults (operating shutdown). The proposed power conversion of the PV panels used in this work is shown in Fig 3.4. Interleaved boost converter (IBC) has been introduced in the literature, including 2-phase, 3-phase and 4-phase [157-159]. The interleaved topology provides different features as: (i) minimize the size and volume of passive components; (ii) reduce the Input ripple current ;(iii) increase the frequency of the input current; (iv) improve the reliability of the system due to the higher voltage gain; (v) Increase the output power of the converter due to the parallel phases; (vi) Provide simple thermal management, the parallel of IBC and IBDC converters phases allow a better thermal distribution The IBC, in this type of assembly's inductors, switches and diodes are connected in parallel; a single capacitor is placed at the output of the converter. The control of the switches S_1 , S_2 ,, and S_n is successively shifted by T_s/N ; T_s is the switching period, N is the number of branches constituting the converter.

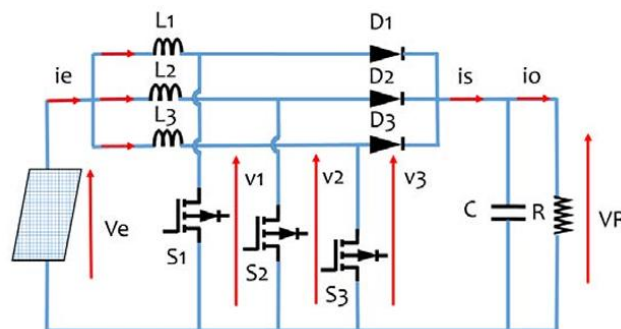


Fig 2: Interleaved (DC/DC) Converter.

Table 1 charging system component parameters.

Parameter Description	Value
Rated DC Bus Voltage	750V
DC Charger Power	45kW
PV Power Capacity	100kW

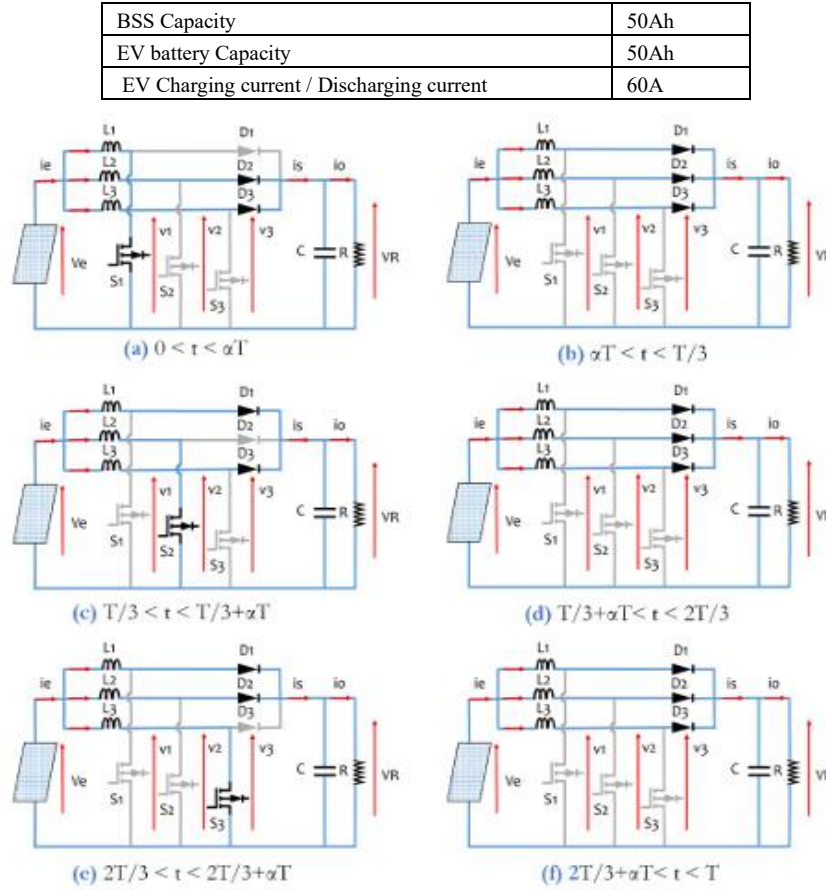


Fig. 3: Behavior of interleaved converter in each small interval

The switching sequences of the switches may or may not overlap, causing variations in the ripple of the input current. The frequency of the input current is N times the frequency of the current in each inductance [160, 161]. The analysis of the voltage ripples and the current according to the duty cycle is obtained under the following simplifying assumptions: 1. The resistances of the coils and the capacitor are negligible. 2. Inductances and parasitic capacitances are negligible. 3. Switches are ideal. The equations of the proposed circuit of IBC converter depicted in Fig 3 are:

$$V_1 = L_1 \frac{di_1}{dt} + V_e$$

$$V_2 = L_2 \frac{di_2}{dt} + V_e$$

$$V_3 = L_3 \frac{di_3}{dt} + V_e$$

The inductances for IBC circuit are identical

$$L_1 = L_2 = L_3 = L.$$

Therefore: $-ie = i_1 + i_2 + i_3$

$$V_1 + V_2 + V_3 = 3V_e - L(di/dt)$$

Control Operation of Power Converters

Various characteristics measured from the DC bus and the car connected to the charging station are used to manage the switching sequence of all the power electronic converters. The voltage and current measured from the PV side are used to drive the MPPT DC-DC converter. Various characteristics measured from the DC bus and the car connected to the charging station are used to manage the switching sequence of all the power electronic converters. The voltage and current measured from the PV devices are used to drive the MPPT DC-DC converter on the PV side. The buck/boost converter to be managed on the BEV side depends on the battery's current draw and charge level. The PV apparatuses. The buck/boost converter to be managed on the BEV side depends on the battery's current draw and charge level. Battery Charging Controller for BEVs Battery Charging Controller for BEVs Constant-voltage and constant-current control are applied to the charging converter in order to charge the BEV battery. Inner current loop control facilitates fast charging, while outer voltage loop control Constant-voltage and constant-current control are applied to the charging converter in order to charge the BEV

battery. Inner current loop control facilitates fast charging, while Figure 4 illustrates the use of outer voltage loop control for constant-voltage charging. The battery is charged when the current entering it is positive ($I_{batt} > 0$); if not, it is discharged. The EMS controller is supplying the battery with a regulated supply based on the battery current's sign (I_{ref}).

RESULTS

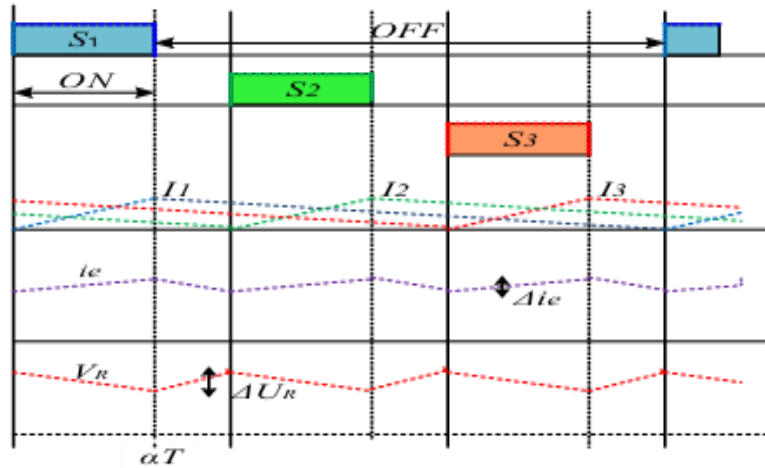


Fig 4: Waveforms of different signals, case 1.

Each interval of $T/3$ can be sub-divided into two intervals to determine the input current, based on equation (3.6, 3.7). Therefore, the equivalent circuit diagrams for each interval are given in Fig 3.6. Only one switch $S3$ is in a conducting mode for each first phase of a $1/3$ of the switching period. The voltage ($V1+V2+V3$) is alternatively equivalent to $2V_R$ and $3V_R$. Defining $i_{e \min}$ as the value of i_e for $t = 0$.

For each conduction interval, $\alpha < 1/3$, the input current of each interval is given by the equations .

Each switch has a conduction time greater than $T/3$ and less than $2T/3$. The timing of the switch's conduction is shown in Fig 3.8. If αT is assumed to be equal to $(\alpha T - T/3)$, and considering the intervals $[0, \alpha T]$, $[T/3, T/3 + \alpha T]$ and $[2T/3, 2T/3 + \alpha T]$, the two switches are conducted in each first phase of a $1/3$ switching period. The voltage ($V1+V2+V3$) is alternatively equivalent to V_R and $2V_R$, therefore the frequency of i_e , is three times of the switch's frequency. Thus, the equivalent circuit diagrams for each interval are given in Fig 3.9. In this case the switches have a longer conduction time than $2T/3$. The conducting time of the switches is given in Fig 3.11. Assuming αT is equal to $(\alpha T - 2T/3)$, and considering the intervals $[0, \alpha T]$, $[T/3, T/3 + \alpha T]$ and $[2T/3, 2T/3 + \alpha T]$, it is observed that three switches are driving in each $1/3$ first phase during the switches time. The voltages ($V1+V2+V3$) are alternating between 0 and V_R . The frequency of current i_e , is equal to three times the switching frequency.

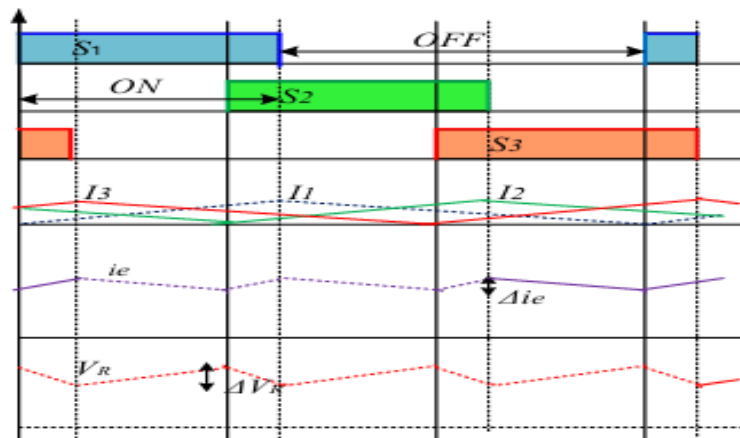


Fig 5: Waveforms of different signals, case 2.

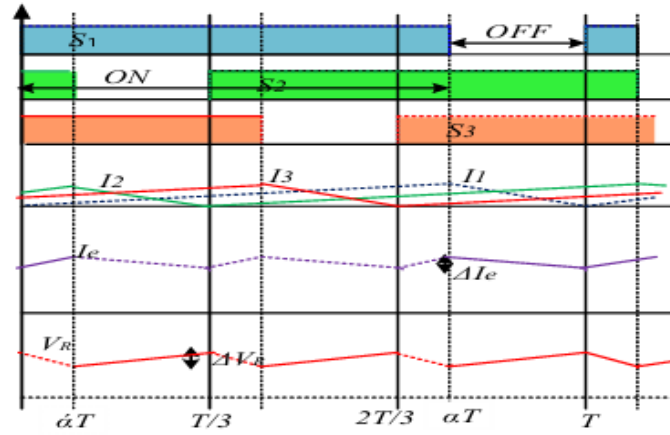


Fig 6: Waveforms of different signals, case 2.

CONCLUSION

In this research work, for PV system, an interleaved DC/DC converter is utilized to maximize the power being harnessed from solar profile. In this case, the interleaved converter also provides regulated voltage at the output. For the BSS, a bidirectional interleaved DC/DC converter topology is proposed and implemented to support the bidirectional power flow and to keep the necessary power balance. At the grid side, a rectifier/inverter conversion stage is implemented to keep the DC bus at regulated value and to support 69 bidirectional power flow between the grid and other components of the hybrid power sources. The main objectives of the power conversion phase are regulating the DC bus at desired value, maintaining the power flow between the connected sources with high efficiency, keeping an overall power quality profile in term of harmonics.

REFERENCES

1. R. K. Lenka, A. K. Panda, A. R. Dash, L. Senapati, and N. Tiwary, "A unified control of grid-interactive off-board EV battery charger with improved power quality," *IEEE Transactions on Transportation Electrification*, vol. 9, no. 1, pp. 920–933, 2023.
2. V. Bist and B. Singh, "PFC Cuk converter-fed BLDC motor drive," *IEEE Transactions on Power Electronics*, vol. 30, no. 2, pp. 871–887, 2015.
3. S. Singh and B. Singh, "A voltage-controlled PFC Cuk converter-based PMBLDCM drive for air-conditioners," *IEEE Transactions on Industry Applications*, vol. 48, no. 2, pp. 832–838, 2012.
4. L. Schrittwieser, J. W. Kolar, and T. B. Soeiro, "99% efficient three-phase buck-type SiC MOSFET PFC rectifier minimizing life cycle cost in DC data centers," *CPSS Transactions on Power Electronics and Applications*, vol. 2, no. 1, pp. 47–58, 2017.
5. J. Garcia, M. A. Dalla-Costa, A. L. Kirsten, D. Gacio, and A. J. Calleja, "A novel flyback-based input PFC stage for electronic ballasts in lighting applications," *IEEE Transactions on Industry Applications*, vol. 49, no. 2, pp. 769–777, 2013.
6. V. C. Sekhar and N. Vishwanathan, "Reduced ripple current led driver with reduced output filter capacitance," in *2021 National Power Electronics Conference (NPEC)*, 2021, pp. 1–6.
7. T. B. Soeiro, T. Friedli, and J. W. Kolar, "Design and implementation of a three-phase buck-type third harmonic current injection PFC rectifier SR," *IEEE Transactions on Power Electronics*, vol. 28, no. 4, pp. 1608–1621, 2013.
8. H. Choi, "Interleaved boundary conduction mode (BCM) buck power factor correction (PFC) converter," *IEEE Transactions on Power Electronics*, vol. 28, no. 6, pp. 2629–2634, 2013.
9. J. Rodriguez, J. Dixon, J. Espinoza, J. Pontt, and P. Lezana, "PWM regenerative rectifiers: state of the art," *IEEE Transactions on Industrial Electronics*, vol. 52, no. 1, pp. 5–22, 2005.
10. A. R. Paul, A. Bhattacharya, and K. Chatterjee, "A single-phase grid-connected boost/buck-boost-derived solar PV micro-inverter topology having power decoupling capability," *IEEE Journal of Emerging and Selected Topics in Power Electronics*, vol. 11, no. 2, pp. 2340–2349, 2023.
11. T. B. Soeiro, T. Friedli, and J. W. Kolar, "Swiss rectifier — A novel three-phase buck-type PFC topology for electric vehicle battery charging," in *Twenty-Seventh Annual IEEE Applied Power Electronics Conference and Exposition (APEC)*, 2012, pp. 2617–2624.
12. M. Pourmahdi, H. Heydari-doostabad, R. Ghazi, and T. O'Donnell, "Buck-boost common ground bridgeless PFC (CGBPFC) rectifies with positive/negative output," *IEEE Transactions on Power Electronics*, vol. 37, no. 2, pp. 1272–1282, 2022.
13. S. Sharifi, M. Monfared, and M. Babaei, "Ferdowsi rectifiers-single-phase buck-boost bridgeless PFC rectifiers with low semiconductor count," *IEEE Transactions on Industrial Electronics*, vol. 67, no. 11, pp. 9206–9214, 2020.
14. M. MahmoodSaleh and E. Adib, "Soft-switching bridgeless buck-boost PFC converter using single magnetic core," *IEEE Transactions on Industrial Electronics*, vol. 68, no. 7, pp. 5704–5711, 2021.
15. M. Jalhotra, L. K. Sahu, S. Gupta, and S. P. Gautam, "Highly resilient fault-tolerant topology of single-phase multilevel inverter," *IEEE Journal of Emerging and Selected Topics in Power Electronics*, vol. 9, no. 2, pp. 1915–1922, 2021.

15. G. Durgasukumar and M. K. Pathak, "THD reduction in performance of multi-level inverter fed induction motor drive," in *India International Conference on Power Electronics 2010 (IICPE2010)*, 2011, pp. 1–6.
 - A. Jain, K. K. Gupta, S. K. Jain, and P. Bhatnagar, "A bidirectional five-level buck PFC rectifier with wide output range for EV charging application," *IEEE Transactions on Power Electronics*, vol. 37, no. 11, pp. 13 439–13 455, 2022.
16. Jain, R. Agarwal, K. K. Gupta, and S. K. Jain, "A V2G-enabled seven-level buck PFC rectifier for EV charging application," in *2022 24th European Conference on Power Electronics and Applications (EPE'22 ECCE Europe)*, 2022, pp. 1–10.
17. J.-i. Itoh, Y. Noge, and T. Adachi, "A novel five-level three-phase PWM rectifier with reduced switch count," *IEEE Transactions on Power Electronics*, vol. 26, no. 8, pp. 2221–2228, 2011.
18. N. Yalla, N. Babu A, and P. Agarwal, "A new three-phase multipoint clamped 5L-HPFC with reduced PSD count and switch stress," *IEEE Transactions on Industrial Electronics*, vol. 67, no. 4, pp. 2532–2543, 2020.